



Cite this: *Soft Matter*, 2017, 13, 4029

## Effect of the material properties on the crumpling of a thin sheet

Mehdi Habibi,<sup>a</sup> Mokhtar Adda-Bedia<sup>c</sup> and Daniel Bonn<sup>a</sup>

While simple at first glance, the dense packing of sheets is a complex phenomenon that depends on material parameters and the packing protocol. We study the effect of plasticity on the crumpling of sheets of different materials by performing isotropic compaction experiments on sheets of different sizes and elasto-plastic properties. First, we quantify the material properties using a dimensionless foldability index. Then, the compaction force required to crumple a sheet into a ball as well as the average number of layers inside the ball are measured. For each material, both quantities exhibit a power-law dependence on the diameter of the crumpled ball. We experimentally establish the power-law exponents and find that both depend nonlinearly on the foldability index. However the exponents that characterize the mechanical response and morphology of the crumpled materials are related linearly. A simple scaling argument explains this in terms of the buckling of the sheets, and recovers the relation between the crumpling force and the morphology of the crumpled structure. Our results suggest a new approach to tailor the mechanical response of the crumpled objects by carefully selecting their material properties.

Received 18th December 2016,  
 Accepted 3rd May 2017

DOI: 10.1039/c6sm02817a

rsc.li/soft-matter-journal

## 1 Introduction

Crumpling and folding of slender objects are ubiquitous phenomena: paper compaction into a ball,<sup>1</sup> cortical folding in mammalian brains,<sup>2</sup> DNA packing in viral capsids,<sup>3,4</sup> flower buds<sup>5</sup> and crumpled graphene<sup>6</sup> are different realizations of this common process. Crumpling a sheet of paper results in a very light structure (with more than 80% void) with a complex fractal topology,<sup>7</sup> surprising mechanical strength and the ability to absorb mechanical energy.<sup>8,9</sup> These peculiar mechanical properties make crumpled sheets a strong candidate for designing robust mechanical metamaterials: disordered crumpled structures – in contrast to *e.g.* ordered origami structures – benefit from inherent insensitivity to noise and defects which can result in superior mechanical functionality for real-world applications. However, a number of key fundamental questions about crumpled structures still need to be addressed before their potential can be fully exploited.

Previous studies<sup>8–15</sup> have shown that the applied force for crumpling a thin plate show a power law dependence on the size of the crumpled object ( $F \sim D^{-\beta}$ ), with an exponent that depends on the material properties, compaction protocol and

self-avoidance constraints. These different effects are difficult to disentangle in spite of extensive experimental,<sup>10,13–18</sup> theoretical<sup>19–25</sup> and numerical<sup>11,12,26–28</sup> studies. Various aspects of the crumpling mechanism are still elusive or controversial, and a general physical understanding is lacking. The difficulties arise from the fact that crumpling involves the formation of a complex network of localized folds<sup>21,22,24</sup> where plastic deformations take place in addition to self-avoiding interactions and jamming effects.<sup>23</sup>

Most materials exhibit an elasto-plastic mechanical response to externally applied stresses and the slenderness of sheets enhances this behavior by localizing stretching deformations in small plastic regions along creases; these remain clearly visible if one unpacks a crumpled paper ball. The effect of plasticity on the crumpling process is still heavily debated.<sup>8,11–13,17,29,30</sup> Ref. 17 suggests that the material properties have only a minor effect. Numerical simulations of 3D isotropic compaction of thin sheets predict that, the self-avoidance is the primary source of resistance against the crumpling force in a way the crumpling exponent ( $\beta$ ) is expected to be universal at values 8/3, and 4, respectively, for sheets that can and cannot cross themselves in the course of compaction, independent of the material properties. Further numerical studies on the effect of plasticity on the compaction of thin sheets show that while the material plasticity results in different morphologies and fractal dimensions when compared to purely elastic systems, the force necessary for crumpling behaves similarly in the two systems<sup>12</sup> with a crumpling exponent of about 3.8. However experimental studies of the crumpling reveal that

<sup>a</sup> Institute of Physics, van der Waals-Zeeman Institute, University of Amsterdam, Science Park 904, 1098 XH Amsterdam, The Netherlands

<sup>b</sup> Laboratory of Physics and Physical Chemistry of Foods, Wageningen University, Wageningen, The Netherlands. E-mail: mehdi.habibi@wur.nl

<sup>c</sup> Laboratoire de Physique, Ecole Normale Supérieure de Lyon, F-69342 Lyon, France

the crumpling exponent is larger than the predicted universal values and is material-dependent, changing from 5.1 to 15.4 for the aluminum foil and polymer sheets, respectively.<sup>13,29</sup> On the other hand, ref. 8 argues that crumpling can be viewed as arising from successive folding events and show that predictions from simple folding models can capture many of the complicated features of the crumpling process. Since the mechanism of folding depends sensitively on the mechanical properties, very different behaviors are predicted for elastic and perfectly plastic sheets. Furthermore, a recent MD simulation of the crumpled sheets predicts plasticity dependent morphological properties with a universal plasticity independent crumpling exponent of 4.5.<sup>30</sup>

In this article, we systematically study the effect of the material properties on the crumpling process to investigate the differences between the crumpling of elastic and plastic materials. This is done by performing isotropic compression of sheets of various materials with very different elasto-plastic mechanical responses. First, we introduce a simple procedure that allows us to characterize the plasticity of a slender material through a dimensionless parameter referred to as the foldability index. Then we quantify the crumpling process by performing experimental measurements of the crumpling force and the number of layers as a function of the size of the crumpled ball. For all samples, the force and number of folds exhibit non-trivial power law behaviors with exponents that decrease with increasing plasticity of the material. However the force and number of layers of the exponents are simply linearly related, showing the pertinence of the folding model, and allowing us to quantify the effect of plasticity with a single parameter: the foldability index. Knowledge of this independently measurable parameter then allows us to quantitatively predict the complicated and highly non-linear compaction process.

## 2 Experiments

### (a) Plasticity measurements

To cover a wide range of mechanical responses, different materials: PDMS rubber membranes (with thickness  $h = 1$  mm), Mylar ( $h = 75, 36, 23,$  and  $19$   $\mu\text{m}$ ), regular printing paper ( $h = 100$   $\mu\text{m}$ ) and aluminum foil ( $h = 8$  and  $20$   $\mu\text{m}$ ) are used. To quantitatively measure plasticity we introduce a novel method, in which an initially flat, thin ribbon of the material is rolled (one round) around a cylinder of radius  $R_c$  (ranging from 1 to 50 mm) under a constant extensional load (see Fig. 1a). The rolled ribbon is kept under tension for about 30 minutes (comparable to the maximum relaxation time of the materials used<sup>13,31</sup>) and then released. Unloading the system results in a rapid unwinding of the ribbon followed by a gradual relaxation. After about one hour the curved ribbon reaches its final radius  $R_f$  (see Fig. 1b). Fig. 1c shows the dimensionless curvature of the ribbon ( $h/R_f$ ) as a function of the dimensionless curvature of the cylinder ( $h/R_c$ ) for different materials and for specific ranges of curvatures that overlap with the crease deformations that are obtained in crumpled structures.  $h/R_f$  shows a power-law dependence on  $h/R_c$  with an exponent that decreases with increasing

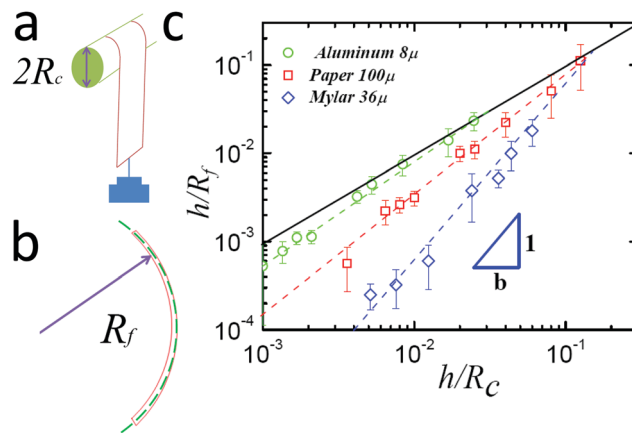


**Fig. 1** (a) A flat, thin ribbon of the material under study (2 cm in width) is rolled around a cylinder of radius  $R_c$  (ranging from 1 to 50 mm) under a constant extensional load of 1 kg for about 30 minutes and then released. (b) The unloaded ribbon reaches a final radius of curvature  $R_f$ . (c) Dimensionless curvature  $h/R_f$  of three types of ribbons (aluminum foil, paper, Mylar) as a function of the dimensionless curvature of the cylinder  $h/R_c$  on a double logarithmic scale. The black solid line represents an ideal plastic material where  $h/R_c \sim h/R_f$ . The dotted/dashed lines are power-law fits with different exponents. The inverse of the power-law exponent is referred as the foldability index of the material  $b$ . Notice that while the power law behaviour holds for a large range of deformations, the material response deviates from it for extreme cases.

plasticity of the material. Here, the inverse of the power-law exponent is introduced as the foldability index ( $b$ ) of the material:  $h/R_f \sim (h/R_c)^{1/b}$ . For an ideal plastic material one expects  $h/R_c \sim h/R_f$  which gives  $b = 1$ . Fitting power laws to the experimental data in Fig. 1c then yields foldability indexes  $b = 0.86 \pm 0.05$  for aluminum foil,  $b = 0.74 \pm 0.05$  for paper and  $b = 0.55 \pm 0.1$  for Mylar. As we can observe from the results the parameter  $b$  seems to be smaller for the materials that we are used to think as more elastic. However, for a pure elastic material such as PDMS rubber, the final curvature is always zero as the sheet would always unfold independently of the curvature of the cylinder, thus a power law behavior does not hold. This indicates that the foldability index is a parameter that characterizes the state of the system beyond its elastic limit. Indeed, plasticity is normally addressed by the strain for yielding which is a threshold parameter that separates the elastic and plastic behaviors, while  $b$  characterizes the behavior of the material beyond yielding. This behavior is responsible for the mechanical properties of the creases and consequently for both geometrical and mechanical properties of the crumpled structure. Since we are interested in characterizing the geometrical aspects of crumpling thus it is legitimate to have a non-extensive parameter (dimensionless number) such as  $b$ .

### (b) Crumpling experiments

The experimental setup consists of a net of wires distributed uniformly around a loosely crumpled sheet of initial size  $D_0 = 30$  cm, which is fed through a hole underneath the crumpling structure (see Fig. 2). The degree of confinement is increased by sequentially attaching additional weights to the



Fig. 2 (a) Experimental setup consisting of a net of wires distributed uniformly around a loosely crumpled sheet, which pass through a hole in the platform on which the crumpled sheet is placed. (b) By hanging weights at the bottom of the net one achieves higher degree of quasi-isotropic compaction. The scales are 2 cm.

bottom of the net, pulling it down. This setup enables us to apply a quasi-isotropic confinement on the outer surface of the crumpled structure. About 10 minutes after each incremental increase of the load, the crumpled sheet reaches its approximate final size and its size no longer changes significantly. The average size of the ball,  $D$ , and the crumpling force,  $F$ , are recorded. Subsequently, additional weights are attached to the net to increase the crumpling force and achieve a higher level of compaction. The contact points between the wires and the feedthrough hole are lubricated using Silicone oil (100 cSt) to reduce frictional effects.

### 3 Experimental results

#### (a) Crumpling force vs. compaction

In the inset of Fig. 3 the crumpling force  $F$  is plotted as a function of the average crumpled size  $D$  for Mylar sheets of different thicknesses. It shows that the force increases with decreasing size of the crumpled ball as a power-law. We call the power-law exponent the crumpling-force exponent. This exponent for Mylar is approximately the same for all sheet thicknesses. The observed shift for different data sets is due to differences in the initial thickness of the sheets; however the powers are similar. To quantify the sheet thickness effect, we scale the crumpling force by the force needed to make a single fold which from simple elasticity considerations is  $\propto Eh^2$ , where  $E$  is the elastic modulus of the material.<sup>8</sup> The rescaled crumpling-force for all the materials is shown in Fig. 3 which confirms that data points for different material thicknesses indeed collapse onto each other. Moreover, the dependence on the size of the ball is well captured by  $F/Eh^2 \sim (D/D_0)^{-\beta}$  where  $\beta$  is plasticity-dependent. This exponent decreases with increasing plasticity from  $\beta \approx 6$  for rubber membranes to  $\beta \approx 3.9$  for aluminum foil (Fig. 6).

We also find that the force needed to crumple a sheet for the first time ('virgin sheet') is larger than for a sheet that has been crumpled before ('trained sheet') (Fig. 4). This is not surprising, as in general there are two main contributions to the crumpling force: the mechanical response of the crumpled network and

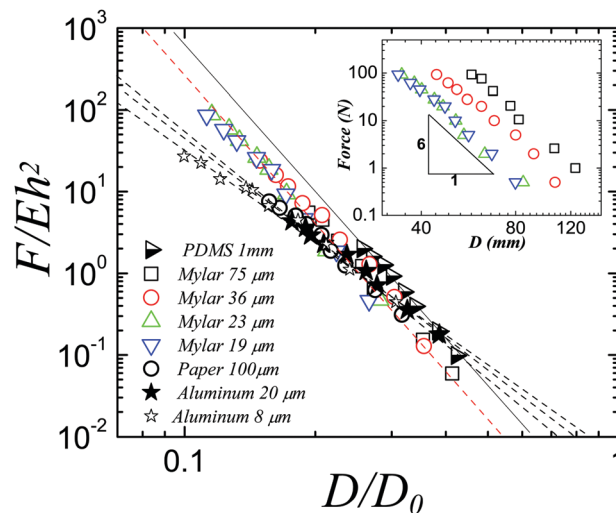


Fig. 3 Dimensionless crumpling force ( $F/Eh^2$ ) as a function of dimensionless average size of crumpled balls ( $D/D_0$ ). The dependence on size of the rescaled crumpling force is captured well by  $F/Eh^2 \sim (D/D_0)^{-\beta}$  with a plasticity-dependent exponent  $\beta$ . The error bars have not been shown for the sake of clarity. The maximum error bar is about 10%. Inset shows the crumpling force  $F$  as a function of the average crumpled size  $D$  for Mylar sheets of different thicknesses.

the force needed for the creation of crease patterns. For trained sheets the only contribution is due to the mechanical response of the crumpled network since most of the crease patterns has already been created. However as shown in Fig. 4, the crumpling-force exponents for virgin and trained sheets are the same within the experimental error, allowing us to conclude that the exponent adequately reflects the mechanical response of the crumpled sheets.

The crumpling exponent  $\beta$  of aluminum foil is in good agreement with the numerical prediction of ref. 12 in which plasticity was taken into account in simulations. However, for

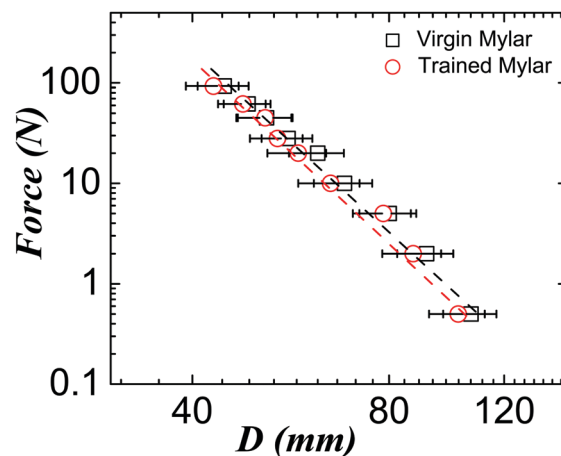


Fig. 4 Crumpling force ( $F$ ) as a function of the average size of crumpled balls ( $D$ ) for Mylar sheets crumpled for the first time ('virgin sheet') and one that has been crumpled before ('trained sheet'). The crumpling-force exponents for the virgin and trained sheets are  $5.76 \pm 0.15$  and  $5.85 \pm 0.15$ , respectively. The thickness of the sheet is  $h = 36 \mu\text{m}$ .

printing paper, we find  $\beta \approx 4.5$  in contrast with the exponent  $\beta \approx 1.5$  found in ref. 8. This discrepancy is explained by the difference in the packing protocol: it is isotropic in the present work while it was unidirectional in ref. 8. Note that our results also contrast with those of ref. 13, where exponents  $\beta$  of 5.1 and 15.4 (instead of 3.9 and 6) were reported for aluminum foil and HDPE sheets, respectively, albeit again using a different experimental procedure. Repeating the procedure of ref. 13 we recovered similar results to those reported in it, and concluded that the exponents also depend on the packing protocol. Indeed, the exponents we obtained here results from the isotropic packing protocol we built: for instance in the experiments of ref. 13 the sheet needs to be pre-crumpled anisotropically and packed by a PVC wrap to a tube connecting to the outside of the pressure chamber which results in a different exponent.<sup>30</sup> Furthermore, their final crumpled structures are not spherical and so the packing is not isotropic.

### (b) Morphology and number of layers

A second step towards understanding the crumpling process is to establish a relation between the degree of compaction and the number of layers in the crumpled configurations.<sup>8</sup> To achieve this, sheets of different materials are crumpled into balls of different degrees of compaction. The number of layers is measured either by counting them along the diameter of a cross-section (by cutting the crumpled ball into two equal parts) or by passing a needle through the crumpled structure and counting the number of holes in the sheet after unfolding it. For the latter technique, the average number of layers,  $N$ , is obtained by repeating this operation in different orientations passing through the center of the ball. Fig. 5 reveals that another power-law dependence is found

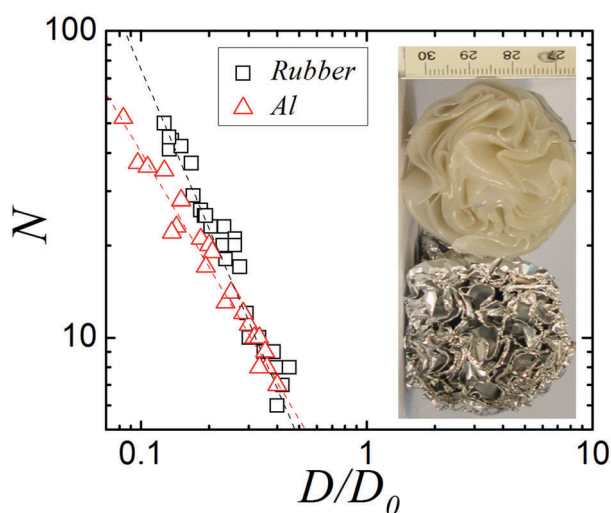


Fig. 5 Variation of the mean number of layers  $N$  with the dimensionless size of crumpled balls ( $D/D_0$ ) for rubber membrane and aluminum foil. Data points for Mylar and paper are not shown for sake of clarity. Dashed lines are power law fits of experimental data. The inset shows cross sections of crumpled sheets of rubber (top) and aluminum foil (bottom) and reveals different stacking behavior. While for aluminum foil the density of layers is larger near the outer surface, the compaction of rubber membrane is more homogeneous.

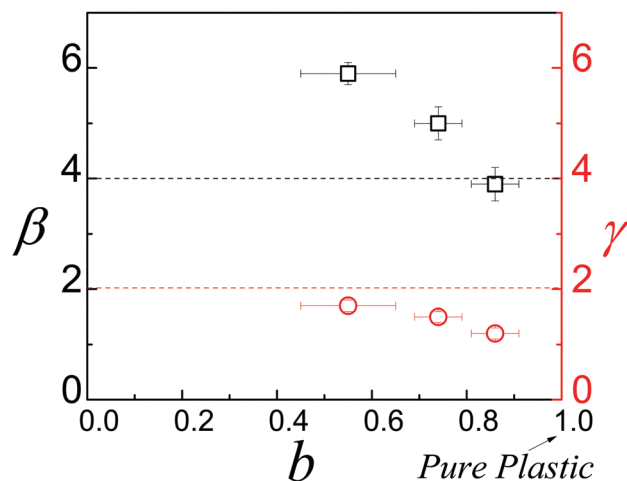


Fig. 6 Crumpling exponent  $\beta$  and layering exponent  $\gamma$  as a function of the foldability index  $b$ . Both exponents are obtained by fitting power laws to the experimental data for different materials. The foldability index is 1 for an ideal plastic material.  $\beta$  and  $\gamma$  exponents for PDMS are 6 and 1.7 respectively. The black and red dotted lines are, respectively, the  $\beta = 4$  and  $\gamma = 2$  predicted by the hierarchical folding model.<sup>8</sup>

for the dependence of the number of folds  $N$  on the size of the crumpled ball:  $N \sim (D/D_0)^{-\gamma}$ . The exponent  $\gamma$  also decreases with increasing plasticity from  $\gamma \approx 1.7$  for rubber to  $\gamma \approx 1.2$  for aluminum foil (Fig. 6). These results should be compared to  $\gamma \approx 2$  predicted by a simple folding model and the experimental results for unidirectionally crumpled paper<sup>8</sup> that gives comparable exponents, but here we are more precise in determining the layering exponent.

Fig. 6 shows the similar trends for both  $\beta$  and  $\gamma$  with foldability index  $b$ . In fact, plotting  $\beta$  as a function of  $\gamma$  for

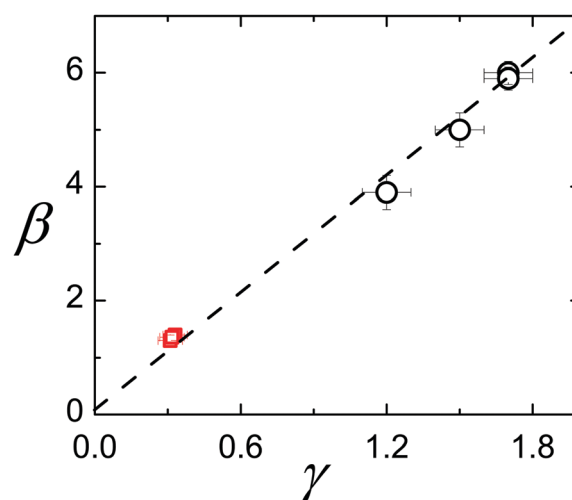


Fig. 7 Crumpling exponent  $\beta$  as a function of layering exponent  $\gamma$  for different materials. Circles are data obtained from the isotropic 3D compaction experiments of PDMS, Mylar, paper and aluminum foil as described here. Squares represent experimental results for quasi 1D compaction of Mylar, paper and aluminum foil in a cylinder. The experimental details for quasi 1D compaction are the same as described in ref. 8. The dashed line with slope 3.44 is the best fit to the data.

the different materials used in this work reveals a linear dependence (Fig. 7). To obtain quasi 1D compaction exponents of Mylar, paper and aluminum foil, the experimental procedure described in ref. 8 was performed. And also these fall on the same line (squares in Fig. 7): here our findings are independent of the details of the compaction process itself. The best fit to all the data (assuming a linear dependence with no offset) gives a slope of  $3.44 \pm 0.1$ .

## 4 Discussion

Considering the fact that the exponent  $\beta$  reflects the mechanical properties of a crumpled structure and the exponent  $\gamma$  its morphology, their proportionality indicates that the morphology and mechanical properties of the folded objects are correlated independently of the material properties. As such, they can be used to tailor the mechanical response of a crumpled structure.

To explain the experimental result  $\beta \approx 3.44\gamma$ , we consider that the crumpling process induces a network of creases that folds the initial thin plate of size  $D_0^2$  into a smaller structure made of  $N$ -facets of characteristic size  $R^2 \sim D_0^2/N$  and characteristic thickness  $H \sim Nh$ . Notice that in contrast with hierarchical folding,<sup>8</sup> one has  $R \neq D$  in a real crumpling process. The mechanical response of the crumpled object is assumed to be mediated by bending deformations of the facets,<sup>32</sup> thus the force needed for the buckling of such a plate is  $F \sim EH^3/R \sim (Eh^3/D_0)N^{7/2}$ . Therefore, these simple scaling arguments yield  $\beta = 3.5\gamma$ , which is in excellent agreement with the experimental results shown in Fig. 7. For hierarchical folding, similar linear relations between folding force and layering exponents were predicted, with coefficients of  $\gamma$  equal to 2, 1 and 1 for 3D, 2D and 1D folding, respectively.<sup>8</sup> These results indicate that the proportionality coefficient between the compaction force exponent and the layering exponent is independent of the material properties but set by the method of compaction (crumpling or folding).

As is well-known from unfolding a crumpled paper ball, plasticity causes irreversible small-curvature creases, which also affect the compaction process. For an ideal elastic sheet, such creases will disappear when higher compactions are achieved, as shown in ref. 33. For plastic materials this is not the case, which causes a shrinkage of the effective area of the sheet, and hence a smaller number of layers at a certain degree of compaction. This is indeed what we observe experimentally (Fig. 5). For aluminum foil the outer layers are more compact than the inner ones, with smaller radii of curvature;<sup>15</sup> for the rubber with the same degree of compaction the compaction is more homogeneous and the average radius of curvature is larger, which together results in smaller values of  $N$  for aluminium than for PDMS at a given degree of compaction. This effect is not taken into account in the above argument for the linear relation between the morphology and force exponents, and could constitute an important refinement.

To fully disentangle the complexity of the crumpling phenomenon one should include the effect of friction between

different layers. Friction does not strongly affect the mechanical response of the crumpled structure at the beginning of the compaction process when different parts of the sheet do not considerably interact yet. However at a high packing fraction, friction plays an important role in the crumpling mechanism and then influences the mechanical response of the crumpled structure.<sup>34</sup> High friction does not allow layers to slide over each other and to reconfigure the structure, which definitely influences the energy dissipation in structures under extreme deformations. In our study we have tried to minimize the effect of friction by limiting our system to sheets with a low friction coefficient and to moderate packing fractions such that the reconfiguration of the crumpled structure was prevalent.

## 5 Conclusion

In conclusion, we investigated the crumpling of sheets of different materials under isotropic compaction and studied the effect of plasticity of the material on the compaction force and resulting morphology. We presented a new geometrical method to characterise the elasto-plastic properties of thin plates and quantify these with a single number. This enables us to quantitatively characterize a series of materials from elastic to very plastic (aluminum foil) through a dimensionless foldability index. We measured the force needed to compact sheets into crumpled balls as well as the average number of layers in the crumpled configuration as a function of confinement. Both quantities were shown to increase with decreasing diameter of the crumpled ball according to power laws, with a plasticity-dependent exponent for each quantity. We found that these exponents are linearly proportional, independently of the material used. The layer thickness of the sheets can also be scaled out in a simple way. Finally, we developed scaling arguments that predict the prefactor of the linear relation, which agrees very nicely with our experiments. These results open the way to tailor the properties of the crumpled materials in such a way that they can be used as robust mechanical metamaterials for shock absorption, mechanical cloaking and as building blocks for more elaborate structures such as light-weight sandwich panels.

## Acknowledgements

We gratefully acknowledge A. D. Cambou and N. Menon for helpful discussions. This work is part of the research program of FOM which is financially supported by NWO. MH acknowledges support from VIDI fellowship from NWO (680-47-548).

## References

- 1 T. Witten, *Rev. Mod. Phys.*, 2007, **79**, 643.
- 2 B. Mota and S. Herculano-Houzel, *Science*, 2015, **349**, 74–77.
- 3 P. K. Purohit, J. Kondev and R. Phillips, *Proc. Natl. Acad. Sci. U. S. A.*, 2003, **100**, 3173–3178.

- 4 E. Katzav, M. Adda-Bedia and A. Boudaoud, *Proc. Natl. Acad. Sci. U. S. A.*, 2006, **103**, 18900–18904.
- 5 H. Kobayashi, B. Kresling and J. F. Vincent, *Proc. R. Soc. London, Ser. B*, 1998, **265**, 147–154.
- 6 J. Baimova, E. Korznikova, S. Dmitriev, B. Liu and K. Zhou, *Rev. Adv. Mater. Sci.*, 2014, **39**, year.
- 7 A. S. Balankin, D. S. Ochoa, I. A. Miguel, J. P. Ortiz and M. Á. M. Cruz, *Phys. Rev. E: Stat., Nonlinear, Soft Matter Phys.*, 2010, **81**, 061126.
- 8 S. Deboeuf, E. Katzav, A. Boudaoud, D. Bonn and M. Adda-Bedia, *Phys. Rev. Lett.*, 2013, **110**, 104301.
- 9 A. S. Balankin, M. M. Cruz, L. A. Caracheo, O. S. Huerta, C. D. Rivas, C. Martinez, D. S. Ochoa, L. M. Ruiz, S. M. Gutiérrez and J. P. Ortiz, *et al.*, *J. Mater. Sci.*, 2015, **50**, 4749–4761.
- 10 K. Matan, R. B. Williams, T. A. Witten and S. R. Nagel, *Phys. Rev. Lett.*, 2002, **88**, 076101.
- 11 G. Vliegthart and G. Gompper, *Nat. Mater.*, 2006, **5**, 216–221.
- 12 T. Tallinen, J. Åström and J. Timonen, *Nat. Mater.*, 2009, **8**, 25–29.
- 13 Y. Lin, Y. Wang, Y. Liu and T. Hong, *Phys. Rev. Lett.*, 2008, **101**, 125504.
- 14 H. Aharoni and E. Sharon, *Nat. Mater.*, 2010, **9**, 993–997.
- 15 A. D. Cambou and N. Menon, *Proc. Natl. Acad. Sci. U. S. A.*, 2011, **108**, 14741–14745.
- 16 D. L. Blair and A. Kudrolli, *Phys. Rev. Lett.*, 2005, **94**, 166107.
- 17 A. S. Balankin, I. C. Silva, O. A. Martinez and O. S. Huerta, *Phys. Rev. E: Stat., Nonlinear, Soft Matter Phys.*, 2007, **75**, 051117.
- 18 A. S. Balankin, A. H. Rangel, G. G. Pérez, F. G. Martinez, H. S. Chavez and C. L. Martinez-González, *Phys. Rev. E: Stat., Nonlinear, Soft Matter Phys.*, 2013, **87**, 052806.
- 19 A. Lobkovsky, S. Gentges, H. Li, D. Morse and T. Witten, *Science*, 1995, **270**, 1482.
- 20 M. Das, A. Vaziri, A. Kudrolli and L. Mahadevan, *Phys. Rev. Lett.*, 2007, **98**, 014301.
- 21 E. M. Kramer and T. A. Witten, *Phys. Rev. Lett.*, 1997, **78**, 1303.
- 22 T. Witten, *Rev. Mod. Phys.*, 1998, **70**, 1531.
- 23 E. Sultan and A. Boudaoud, *Phys. Rev. Lett.*, 2006, **96**, 136103.
- 24 M. B. Amar and Y. Pomeau, *Proc. R. Soc. London, Ser. A*, 1997, 729–755.
- 25 J. Najafi, N. Stoop, F. Wittel and M. Habibi, *Phys. Rev. E: Stat., Nonlinear, Soft Matter Phys.*, 2012, **85**, 061108.
- 26 N. Stoop, J. Najafi, F. K. Wittel, M. Habibi and H. Herrmann, *Phys. Rev. Lett.*, 2011, **106**, 214102.
- 27 J. Åström, J. Timonen and M. Karttunen, *Phys. Rev. Lett.*, 2004, **93**, 244301.
- 28 T. Tallinen, J. Åström and J. Timonen, *Phys. Rev. Lett.*, 2008, **101**, 106101.
- 29 W. Bai, Y.-C. Lin, T.-K. Hou and T.-M. Hong, *Phys. Rev. E: Stat., Nonlinear, Soft Matter Phys.*, 2010, **82**, 066112.
- 30 S.-F. Liou, C.-C. Lo, M.-H. Chou, P.-Y. Hsiao and T.-M. Hong, *Phys. Rev. E: Stat., Nonlinear, Soft Matter Phys.*, 2014, **89**, 022404.
- 31 B. Thiria and M. Adda-Bedia, *Phys. Rev. Lett.*, 2011, **107**, 025506.
- 32 G. Seizilles, E. Bayart, M. Adda-Bedia and A. Boudaoud, *Phys. Rev. E: Stat., Nonlinear, Soft Matter Phys.*, 2011, **84**, 065602.
- 33 A. Pocheau and B. Roman, *Eur. Phys. J. E: Soft Matter Biol. Phys.*, 2014, **37**, 1–15.
- 34 P. Mellado, S. Cheng and A. Concha, *Phys. Rev. E: Stat., Nonlinear, Soft Matter Phys.*, 2011, **83**, 036607.